

Description of elastic polarized-deuteron scattering in the optical model with Skyrme forces

V. V. Pilipenko* and V. I. Kuprikov

National Science Center “Kharkov Institute of Physics and Technology”, 1 Akademichna Street, Kharkov 61108, Ukraine

(Received 3 April 2015; revised manuscript received 17 June 2015; published 14 July 2015)

Microscopic deuteron-nucleus optical potential was constructed on the basis of the nucleon-nucleus optical potentials recently obtained by the authors from approximate calculations of the mass operator of the single-particle Green function using the Skyrme forces, which in general involve additional density- and momentum-dependent terms. Both the nucleon- and deuteron-nucleus elastic scattering processes are described in a self-consistent approach using the effective nucleon-nucleon forces, which simultaneously provide a satisfactory description of nuclear structure. The calculations performed using the Watanabe-type approximation have made it possible to obtain reasonable results for describing differential cross sections and polarization observables for the elastic deuteron scattering in a wide range of target-nucleus mass numbers at different incident deuteron energies, when using several Skyrme-force variants both from literature and proposed by the authors. Contributions to elastic deuteron-nucleus scattering cross sections coming from the effects of deuteron virtual breakup have been estimated in the continuum-discretized coupled channels approach.

DOI: [10.1103/PhysRevC.92.014616](https://doi.org/10.1103/PhysRevC.92.014616)

PACS number(s): 24.10.Ht, 25.45.-z, 21.30.Fe, 21.60.Jz

I. INTRODUCTION

Development of a unified theory that would include both the shell model of atomic nuclei and the microscopic optical potentials (MOP) of the interaction of nucleons and light nuclei, in particular deuterons, with nuclei is of considerable interest. At the present time, different models of MOP for describing nuclear scattering processes are developed, which are based on using various effective nucleon-nucleon (NN) forces and realistic nuclear densities. Among the frequently used approaches are the folding models (see, for example, [1–3]). For describing the deuteron scattering at energies of about several tens of MeV, the three-body $n + p + A$ models are also used of the Watanabe folding type [4–7] and of the Faddeev-like type with nonlocal and local optical potentials [8,9]. The continuum-discretized coupled channels (CDCC) method should be mentioned, which was successfully employed for studying the deuteron-nucleus (dA) scattering and reactions in a wide energy range during recent decades [10–13]. The CDCC formalism is a three-body approach, which describes the dA interaction, as in the Watanabe model, in terms of the nucleon-target optical potentials but explicitly includes effects of the deuteron virtual breakup channels, which can be important for such weakly bound projectiles as deuterons. We also mention the approach to describing the dA interaction developed in Refs. [14–17], which is based on nonlocal optical potentials and was employed for analyzing the deuteron stripping reactions on nuclei. In Refs. [16,17] the connection between the three-body model and the underlying many-body problem is discussed.

Starting from Ref. [18], extensive investigations have been devoted to the elaboration of effective NN forces of the Skyrme type, which are widely used in microscopic calculations of nuclear structure and properties of nuclear matter. At the present time, much attention is given to the problem of searching for Skyrme-type NN forces (see, for

example, Ref. [19] and references therein) which could be simultaneously applicable for describing different properties of nuclei, in particular, of exotic ones, the properties of excited states of nuclei, including giant resonances, and for astrophysical problems, such as calculations of neutron stars. In this connection, it is also of interest to extend the field of application of the Skyrme forces to the description of nuclear scattering processes.

For this purpose in Refs. [20–26], an approach to analyzing NA scattering was developed in which for finding the corresponding NA optical potentials approximate calculations of the mass operator of the one-particle Green function were employed. In our papers [22–24], the real part of the NA MOP was used in the form of the finite-nucleus potential, calculated in the Hartree-Fock approximation with the Skyrme forces (SHF) of the standard form [18]. In the calculations of the imaginary part of the MOP, which were performed in the nuclear matter approximation, we used the dispersion law also with the SHF potential for finite nuclei. It should be emphasized that in Refs. [22–26], in contrast to Refs. [20,21], the self-consistent calculations of the NA MOP and nucleon densities of the target nucleus were used. In the work of Ref. [25], the approach [22–24] was employed to find the NA MOP on the basis of the extended variants of Skyrme forces with the allowance for both the density- and momentum-dependent terms of the type used in Refs. [27–29]. The analysis of the neutron- and proton-nucleus scattering allowed us to find some new sets of parameters of the Skyrme forces of the standard and extended forms, which provide a satisfactory description of differential cross sections and analyzing powers of the elastic scattering of medium-energy nucleons on different target nuclei as well as of the reaction and total interaction cross sections. Moreover, the use of certain variants of the extended Skyrme forces yielded a somewhat better description of experimental data. In view of the promising results of this approach in analyzing the NA scattering using the simultaneous self-consistent description of nuclear structure employing the same Skyrme forces, it seems expedient to spread such an approach for constructing MOP for

*vpilipenko@kipt.kharkov.ua

the deuteron-nucleus (dA) scattering. Here, we will consider the use of dA MOP constructed in the three-body $n + p + A$ model basing on the NA optical potentials obtained in the above self-consistent approach.

In Ref. [30], it was shown that the dA MOP can be identified with the mass operator of the two-particle Green function in the nuclear medium. After ignoring the contributions which go beyond the three-body model and neglecting the effects of deuteron breakup, the considered model became analogous to the Watanabe model [4]. As a result, in Ref. [30] the dA optical potential was represented in the folding form with employing the NA optical potentials from the model of Ref. [20] calculated on the basis of the Skyrme forces in the approximations of nuclear matter and local density, and this dA MOP was used for analyzing the experimental elastic dA scattering cross sections. Note that in Refs. [16,17] it was pointed out that there is a problem of investigating the role of the terms going beyond the three-body model, whose quantitative significance is not yet exactly known.

In our work of Ref. [31], the analysis of the dA scattering cross sections was performed basing on an analogous Watanabe-type model, but with employing a more sophisticated model of the NA MOP from Refs. [22–24], which were calculated in the self-consistent approach with the standard Skyrme forces. In the present work, this model of the dA MOP is further developed for using the Skyrme forces of the above-mentioned extended form. The applicability of various standard and extended Skyrme forces for describing the dA scattering is investigated, including the optimized variants of NN forces found by the authors in Refs. [25,26] from analyzing the elastic NA scattering observables and characteristics of nuclear structure. We complement the analysis of the dA elastic scattering differential cross sections by calculations of various polarization observables, which were not considered in Refs. [30,31]. Because deuteron is a weakly bound nucleus, it is also interesting to assess the effects of its virtual breakup upon description of the dA scattering, which also were not studied in Refs. [30,31] and here are estimated using the CDCC approach.

II. THE MODEL OF dA MICROSCOPIC OPTICAL POTENTIAL WITH THE EXTENDED SKYRME INTERACTION

Let us consider the scheme of constructing the MOP for describing the dA scattering on the basis of the model of NA MOP developed by us earlier in Refs. [22–26], which is based on calculations of the mass operator of the one-particle Green function with using the Skyrme forces depending on the nuclear density. As in Ref. [30], we use the approximations that make the dA MOP calculation scheme analogous to the Watanabe model [4], which was used by many authors for describing scattering of composite particles by nuclei.

The Schrödinger equation for the scattering of the two-nucleon system on an atomic nucleus can be written in the

three-body model in the form,

$$\left\{ -\frac{\hbar^2}{2M_d} \frac{\partial^2}{\partial \mathbf{R}^2} + \hat{H}_{\text{in}}(\mathbf{r}) + \hat{U}_1(\mathbf{r}_1) + \hat{U}_2(\mathbf{r}_2) - \varepsilon \right\} \times \Psi(\mathbf{R}, \mathbf{r}; \sigma_1, \sigma_2; \tau_1, \tau_2) = 0. \quad (1)$$

Here $\Psi(\mathbf{R}, \mathbf{r}; \sigma_1, \sigma_2; \tau_1, \tau_2)$ is the wave function of two incident nucleons; $\mathbf{r} = \mathbf{r}_1 - \mathbf{r}_2$ and $\mathbf{R} = (\mathbf{r}_1 + \mathbf{r}_2)/2$ are the radius vectors of their relative motion and of the center of mass of this system, where \mathbf{r}_1 and \mathbf{r}_2 are the radius vectors of these nucleons being measured from the target-nucleus position; σ_1, σ_2 and τ_1, τ_2 are the spin and isospin variables of these nucleons. In Eq. (1), ε is the energy of the system; $M_d = 2mM/(M + 2m)$ is the reduced mass of the deuteron-nucleus system, where m and M are the masses of nucleon and target nucleus. The Hamiltonian of the internal motion of the two-nucleon system has the form:

$$\hat{H}_{\text{in}}(\mathbf{r}) = -\frac{\hbar^2}{2\tilde{m}} \frac{\partial^2}{\partial \mathbf{r}^2} + V_{12}(\mathbf{r}), \quad (2)$$

where $\tilde{m} = m/2$ is the reduced mass of the two-nucleon system, and $V_{12}(\mathbf{r})$ is the potential of interaction between the nucleons. The optical potentials $\hat{U}_1(\mathbf{r}_1)$ and $\hat{U}_2(\mathbf{r}_2)$ describe the interaction of the first and second nucleons with the target nucleus.

If we neglect the tensor interaction in the potential $V_{12}(\mathbf{r})$, then the wave function of the deuteron ground state can be chosen in the form,

$$\psi_0(r; \sigma_1, \sigma_2; \tau_1, \tau_2) = \varphi_0(r) \chi_{1,\mu}^{(s)}(\sigma_1, \sigma_2) \chi_0^{(\tau)}(\tau_1, \tau_2), \quad (3)$$

where $\varphi_0(r) = u_0(r)/(\sqrt{4\pi}r)$ is the radial wave function of the deuteron; the spin function $\chi_{1,\mu}^{(s)}$ corresponds to the deuteron spin $S = 1$, μ being the deuteron spin projection; the isospin function $\chi_0^{(\tau)}$ corresponds to the zero total isospin of the deuteron. The wave function (3) does not take into account the D -wave admixture in the deuteron ground state and satisfies the equation: $\hat{H}_{\text{in}}\psi_0 = \varepsilon_d\psi_0$, where $\varepsilon_d < 0$, $|\varepsilon_d|$ being the deuteron binding energy. Other states of the two-nucleon system $\psi_i(\mathbf{r}; \sigma_1, \sigma_2; \tau_1, \tau_2)$, $i > 0$, satisfy the equations: $\hat{H}_{\text{in}}\psi_i = \varepsilon_i\psi_i$, with energies $\varepsilon_i > \varepsilon_d$. They are orthogonal to the ground state, $\langle \psi_0 | \psi_i \rangle = 0$, and, together with ψ_0 , form the complete set of states. The wave function of the two-nucleon system in the target-nucleus field can be expanded in terms of this complete set of functions:

$$\Psi(\mathbf{R}, \mathbf{r}; \sigma_1, \sigma_2; \tau_1, \tau_2) = \varphi_0(r) \chi_0^{(\tau)}(\tau_1, \tau_2) \Phi(\mathbf{R}; \sigma_1, \sigma_2) + \sum_{i>0} \psi_i(\mathbf{r}; \sigma_1, \sigma_2; \tau_1, \tau_2) \phi_i(\mathbf{R}). \quad (4)$$

In the first term in Eq. (4), the wave function of the deuteron motion, $\Phi(\mathbf{R}; \sigma_1, \sigma_2)$, is symmetric relative to the permutation of space variables, $\mathbf{r}_1 \leftrightarrow \mathbf{r}_2$, and must also be symmetric relative to the permutation of σ_1 and σ_2 , which corresponds to the total deuteron spin $S = 1$, and therefore it can be expanded in the deuteron spin functions $\chi_{1,\mu}^{(s)}$. The second term in Eq. (4) describes processes of the deuteron breakup in the

target-nucleus field:

$$F(\mathbf{R}, \mathbf{r}; \sigma_1, \sigma_2; \tau_1, \tau_2) = \sum_{i>0} \psi_i(\mathbf{r}; \sigma_1, \sigma_2; \tau_1, \tau_2) \phi_i(\mathbf{R}). \quad (5)$$

It is orthogonal to the ground state: $\langle \psi_0 | F \rangle = 0$.

Taking into account the isotopic invariance of the NA forces in the absence of the Coulomb interaction, we can represent the optical NA potentials in Eq. (1) in the form,

$$\begin{aligned} \hat{U}_i &= U_0(r_i) + U_{LS}(r_i) \mathbf{l}_i \cdot \boldsymbol{\sigma}_i \\ &+ [U_0^{(\tau)}(r_i) + U_{LS}^{(\tau)}(r_i) \mathbf{l}_i \cdot \boldsymbol{\sigma}_i] (\mathbf{T} \cdot \mathbf{t}_i) + \frac{1}{2} (1 - \tau_{i3}) \tilde{V}_C(r_i). \end{aligned} \quad (6)$$

Here \mathbf{l}_i and $\boldsymbol{\sigma}_i$ are the orbital-moment operator and the spin Pauli matrices of the i th scattered nucleon ($i = 1, 2$), and $\mathbf{t}_i = \boldsymbol{\tau}_i/2$ is its isospin operator, where $\boldsymbol{\tau}$ are the isospin Pauli matrices; $\mathbf{T} = \sum_{j=1}^A \mathbf{t}_j$ is the total isospin operator of the target nucleus consisting of A nucleons.

For the NA MOP we shall employ the expressions found by us in Ref. [25] on the basis of calculations with using the effective Skyrme NN interaction of the extended form, which is written as follows:

$$\begin{aligned} V_{ij} &= V(\mathbf{r}, \rho) = t_0(1 + x_0 P_\sigma) \delta(\mathbf{r}) + \frac{1}{2} t_1(1 + x_1 P_\sigma) \\ &\times [\mathbf{k}'^2 \delta(\mathbf{r}) + \delta(\mathbf{r}) \mathbf{k}^2] + t_2(1 + x_2 P_\sigma) \mathbf{k}' \delta(\mathbf{r}) \mathbf{k} \\ &+ \frac{1}{6} t_3(1 + x_3 P_\sigma) \rho^\gamma(\tilde{\mathbf{R}}) \delta(\mathbf{r}) + i W_0(\boldsymbol{\sigma}_1 + \boldsymbol{\sigma}_2) \\ &\times [\mathbf{k}' \times \delta(\mathbf{r}) \mathbf{k}] + \frac{1}{2} t_4(1 + x_4 P_\sigma) [\mathbf{k}'^2 \rho^{\gamma_4}(\tilde{\mathbf{R}}) \delta(\mathbf{r}) \\ &+ \delta(\mathbf{r}) \rho^{\gamma_4}(\tilde{\mathbf{R}}) \mathbf{k}^2] + t_5(1 + x_5 P_\sigma) \mathbf{k}' \rho^{\gamma_5}(\tilde{\mathbf{R}}) \delta(\mathbf{r}) \mathbf{k}. \end{aligned} \quad (7)$$

Here $\mathbf{r} = \mathbf{r}_i - \mathbf{r}_j$ and $\tilde{\mathbf{R}} = (\mathbf{r}_i + \mathbf{r}_j)/2$ are the relative and center-of-mass coordinates of the i th and j th interacting nucleons; $\rho = \rho_n + \rho_p$, ρ_n , and ρ_p are the total, neutron, and proton densities of the target nucleus; $\mathbf{k} = -i\partial/\partial\mathbf{r}$ and $\mathbf{k}' = i\partial/\partial\mathbf{r}'$ are the momentum operators of the relative motion of these nucleons in the initial and final states; P_σ is the operator of spin permutation. The quantities t_n , x_n ($n = 0-5$), γ , γ_4 , γ_5 , and W_0 are the phenomenological parameters characterizing the NN interaction. In Eq. (7), the terms in the first three lines correspond to the standard form of Skyrme force and the last two lines present the momentum- and density-dependent terms with parameters t_4 and t_5 .

The NA optical potential is found from calculations of the mass operator of the one-particle Green function by perturbation theory up to the Goldstone diagrams of the second order, inclusive [20–25]. The best zero approximation for the mass operator is the mean self-consistent Hartree–Fock (HF) potential, which leads to the cancellation of a certain class of important diagrams [32]. In the SHF theory, the variation of the HF functional with the effective nuclear-density-dependent NN forces results in the rise of the so-called rearrangement potential, which is taken into account in our approach [22–26,31], in contrast to that of Refs. [20,21,30]. Note that the rearrangement potential, or differently the saturation potential, plays an important role in ensuring the saturation of the nuclear forces.

In Ref. [25], we obtained concrete expressions for the NA optical potentials $U_q(r)$ for the incident nucleons of sort q

($q = n, p$) in the case of the extended Skyrme forces (7), which are represented as follows:

$$\begin{aligned} U_q(r, E) &= V_q(r, E) + \frac{1}{r} V_{SO,q}(r) (\mathbf{l} \cdot \boldsymbol{\sigma}) \\ &+ i W_q(r, E) + \delta_{q,p} \frac{m_q^*(r)}{m_q} V_C(r), \end{aligned} \quad (8)$$

where the real central part of the NA MOP has the form,

$$\begin{aligned} V_q(r, E) &= \frac{m_q^*(r)}{m_q} [V^{(HF)}(r) + V^{(m)}(r)]_q \\ &+ \left(1 - \frac{m_q^*(r)}{m_q}\right) \frac{M}{M + m_q} E. \end{aligned} \quad (9)$$

Here m_q and E are the mass and laboratory energy of the incident nucleon. The central $V^{(HF)}(r)$, spin-orbit $V_{SO,q}(r)$, and Coulomb $V_C(r)$ potentials are calculated according to the SHF theory for finite nuclei and $m_q^*(r)$ is the effective mass of the nucleon inside the nucleus. The term $V^{(m)}(r)$ arises in the transformation from the nonlocal HF equation to the Schrödinger equation with energy-dependent local potential [33]. The imaginary part of the NA MOP $W_q(r, E)$ arises from the second-order Goldstone diagrams of the perturbation theory and it is calculated in the approximations of nuclear matter and local density. The explicit expressions for all above-mentioned potentials are given in Eqs. (5)–(20) of Ref. [25] and we do not present them here. We only stress that these potentials depend on the densities $\rho_{n,p}(r)$, the kinetic-energy densities $\tau_{n,p}(r)$, and the spin densities $J_{n,p}(r)$ of nucleons [18], which are obtained from the self-consistent calculations of the target-nucleus structure by the SHF method with using the same Skyrme force (for details see Ref. [25]).

In the Watanabe approach [4], we should project the Schrödinger Eq. (1) onto the vector of the deuteron ground state ψ_0 of Eq. (3) and perform averaging over the target-nucleus isospin state $|T, T_3\rangle$, which yields the equation that describes the process of elastic scattering of deuterons by the nucleus:

$$\begin{aligned} \langle \chi_{1,\mu}^{(s)} | \left\{ -\frac{\hbar^2}{2M_d} \frac{\partial^2}{\partial \mathbf{R}^2} + \hat{U}_d(\mathbf{R}) - (\varepsilon - \varepsilon_d) \right\} | \Phi(\mathbf{R}; \sigma_1, \sigma_2) \rangle \\ + \langle \chi_{1,\mu}^{(s)} | G(\mathbf{R}; \sigma_1, \sigma_2) \rangle = 0. \end{aligned} \quad (10)$$

Here the optical potential of dA interaction is determined by the expression:

$$\begin{aligned} \hat{U}_d(\mathbf{R}) &= \langle T, T_3 | \sum_{\tau_1, \tau_2} \chi_0^{(\tau)+}(\tau_1, \tau_2) \int d\mathbf{r} \varphi_0(r) [\hat{U}_1(|\mathbf{R} + \frac{1}{2}\mathbf{r}|) \\ &+ \hat{U}_2(|\mathbf{R} - \frac{1}{2}\mathbf{r}|)] \varphi_0(r) \chi_0^{(\tau)}(\tau_1, \tau_2) | T, T_3 \rangle. \end{aligned} \quad (11)$$

The last term in Eq. (10) corresponds to processes of the virtual breakup of the incident deuteron in the field of the target nucleus and has the following form:

$$\begin{aligned} G(\mathbf{R}; \sigma_1, \sigma_2) &= \langle T, T_3 | \sum_{\tau_1, \tau_2} \chi_0^{(\tau)+}(\tau_1, \tau_2) \int d\mathbf{r} \varphi_0(r) \\ &\times [\hat{U}_1(|\mathbf{R} + \frac{1}{2}\mathbf{r}|) + \hat{U}_2(|\mathbf{R} - \frac{1}{2}\mathbf{r}|)] \\ &\times F(\mathbf{R}, \mathbf{r}; \sigma_1, \sigma_2; \tau_1, \tau_2) | T, T_3 \rangle. \end{aligned} \quad (12)$$

In the Watanabe approximation [4], these latter effects are neglected and the term $G(\mathbf{R}; \sigma_1, \sigma_2)$ is omitted, which leads to the following closed equation for describing the elastic deuteron scattering by the nucleus:

$$\left\{ -\frac{\hbar^2}{2M_d} \frac{\partial^2}{\partial \mathbf{R}^2} + V_{d0}(R) + V_{dC}(R) + V_{d,LS}(R)(\mathbf{L} \cdot \mathbf{S}) + iW_{d0}(R) - E_d^{(\text{cm})} \right\} \Phi(\mathbf{R}; \sigma) = 0. \quad (13)$$

The wave function $\Phi(\mathbf{R}; \sigma)$ depends on the deuteron spin variable $\sigma = \sigma_1 + \sigma_2$, and $E_d^{(\text{cm})}$ is the incident-deuteron energy in the center-of-mass frame of the deuteron-nucleus system. Here the central real and imaginary, the spin-orbit, and the Coulomb parts of the dA MOP are determined by the following formulas [31]:

$$V_{d0}(R) = 2\pi \int_0^\infty dr r^2 |\varphi_0(r)|^2 \int_{-1}^1 du [V_n(r_1, E) + V_p(r_1, E) - (1 - m_p^*(r_1)/m_p) V_C(r_1)], \quad (14)$$

$$W_{d0}(R) = 2\pi \int_0^\infty dr r^2 |\varphi_0(r)|^2 \times \int_{-1}^1 du [W_n(r_1, E) + W_p(r_1, E)], \quad (15)$$

$$V_{d,LS}(R) = \pi \int_0^\infty dr r^2 |\varphi_0(r)|^2 \int_{-1}^1 du [V_{\text{SO},n}(r_1) + V_{\text{SO},p}(r_1)] \frac{1}{r_1} \left[1 + \frac{r}{2R} u \right], \quad (16)$$

$$V_{dC}(R) = 2\pi \int_0^\infty dr r^2 |\varphi_0(r)|^2 \int_{-1}^1 du V_C(r_1). \quad (17)$$

In Eqs. (14)–(17), there are $r_1 = \sqrt{R^2 + \frac{1}{4}r^2 + Rru}$, $u = \cos(\mathbf{Rr})$. The energy of nucleons in the deuteron in Eqs. (14) and (15), as it is made in the majority of works considering dA interaction in the three-body model, is chosen to be $E = \frac{1}{2}E_d$, where E_d is the incident-deuteron energy in the laboratory frame. This choice looks reasonable in the case of elastic scattering in the energy region considered by us, owing to the loose binding of the deuteron, and was also substantiated in Ref. [34] in the framework of the folding dA potential model with using nonlocal NA potentials. However, it may be noted that this prescription can be sometimes not the case, in particular for the (d, p) reactions (see Refs. [14–16]). In the majority of calculations, we used, for the sake of simplicity, the Hulthén form for the deuteron wave function,

$$u_0(r) = \frac{\sqrt{2\alpha\beta(\alpha + \beta)}}{(\beta - \alpha)} [\exp(-\alpha r) - \exp(-\beta r)], \quad (18)$$

with the following values of parameters: $\alpha = 0.23 \text{ fm}^{-1}$, $\beta = 1.62 \text{ fm}^{-1}$.

Note that under the approximations made by us the obtained expressions for the MOP of dA interaction do not contain tensor forces, so that in the calculations of the dA scattering amplitude there is no mixing of partial waves with different values of the orbital moment, as well as the found MOP does not contain a quadratic spin-orbit term.

III. CALCULATIONS OF THE dA SCATTERING OBSERVABLES

On the basis of the above-described Watanabe-like model of dA MOP, which is grounded on the effective Skyrme NN forces of the both standard and extended form, we have developed an original numerical code. Using this code, an analysis was performed of differential cross sections and vector and tensor analyzing powers for the elastic scattering of deuterons with using different variants of the Skyrme forces in the projectile energy region $E_d < 50 \text{ MeV}$ in a wide range of target-nucleus mass numbers. In these calculations, we employed up-to-date variants of the Skyrme forces of both the standard and extended form, which are used in the literature for studying the nuclear structure, as well as the optimized variants SkOP (a standard Skyrme force) and SkOP3 (an extended force with the momentum- and density-dependent terms), obtained by us in Refs. [25,26] by means of variation of the Skyrme force parameters for optimizing the description of the neutron-nucleus scattering with the simultaneous control of values of the main characteristics of the nuclear matter and target-nucleus structure. It should be emphasized that our optimized force variants SkOP and SkOP3 ensured a satisfactory description of the cross sections and polarizations of neutron- and proton-nucleus scattering, which was considerably better than in the cases of using the considered forces from the literature, simultaneously with an acceptable description of characteristics of nuclear structure. Note also that the extended force SkOP3 yielded somewhat better results for the description of NA scattering, than the standard force SkOP.

As an example, in Fig. 1 we present results of calculations of the observables of the elastic $d+^{208}\text{Pb}$ scattering (here and below the numbers in parentheses are the offsetting factor for the cross section and the offset value along the ordinate axis for the analyzing power) at the deuteron energy of 28.8 MeV by the considered model of dA MOP with using our force variants SkOP ($\gamma = 1/6$) and SkOP3 ($\gamma = \gamma_4 = \gamma_5 = 1/3$), as well as with the known from literature standard forces SLy5* ($\gamma = 1/6$) [42], SLyIII.0.8 ($\gamma = 1$) [43], and SAMi ($\gamma \approx 0.256$) [44], and extended forces BSk24 ($\gamma = \gamma_5 = 1/12, \gamma_4 = 1/2$) [45]. All the nucleus-structure calculations in the SHF approach have been performed under the same conditions (the allowance for the center-of-mass motion, exchange Coulomb potential, and spin-orbit interaction), as in the original works for the corresponding force variants. For comparison, here we also present the results of calculations by the analogous Watanabe-type model with using the global NA optical potential CH89 [46]. This global potential is an approved phenomenological approach to describing observables of the elastic NA scattering and, on the whole, yields a better agreement with corresponding experimental data than our NA MOP. Therefore, the comparison of calculations in the considered dA MOP model with using CH89 could be an additional test of applicability of our microscopic NA potential for being employed in the dA scattering calculations.

It can be seen from Fig. 1 that the calculations with our variants SkOP and SkOP3, as well as with the SLy5* force, yield reasonable results being close to each other, although

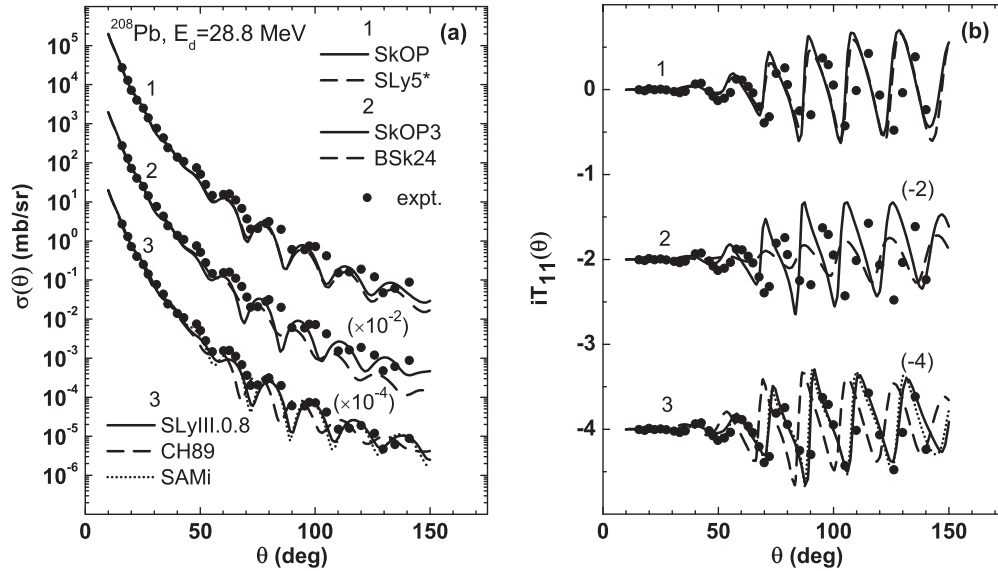


FIG. 1. Differential cross sections $\sigma(\theta) \equiv d\sigma(\theta)/d\Omega$ and vector analyzing powers $iT_{11}(\theta)$ of the elastic scattering of 28.8-MeV deuterons on ^{208}Pb nuclei calculated by the developed model of dA MOP. Experimental data are from Ref. [35].

there is a certain shift of the oscillations of observables towards smaller scattering angles as compared with the experiment. In this concrete case, a somewhat better description of the considered observables was obtained with the forces SLyIII.0.8 and SAMi, the agreement for the analyzing powers being even better than for the cross sections. We may note that the above-mentioned force variants have somewhat different values of the density-dependence exponents but the obtained results do not differ very essentially. Making use of the approved global NA potential CH89 does not give better results in describing the dA scattering observables than the calculations on the basis of these Skyrme forces. The calculations with extended Skyrme force BSk24 have yielded the worst agreement with the data, the results for the all

extended-force variants BSk22–BSk26 from Ref. [45] being somewhat close to each other. Note that the use of the extended force SkOP3, in contrast to the case of NA scattering, does not lead to a considerable improving the description of the dA scattering in the employed model and gives results close to those of calculations with SkOP, which is also the case for other considered target nuclei and deuteron-energy values. For this reason, further we shall consider results of calculations with using the Skyrme force variants SkOP and SLyIII.0.8, comparing them with corresponding calculations with CH89.

In Fig. 2, we present results of such calculations for differential cross sections $\sigma(\theta)$ and vector analyzing powers $iT_{11}(\theta)$ for the elastic deuteron scattering on ^{90}Zr and ^{120}Sn

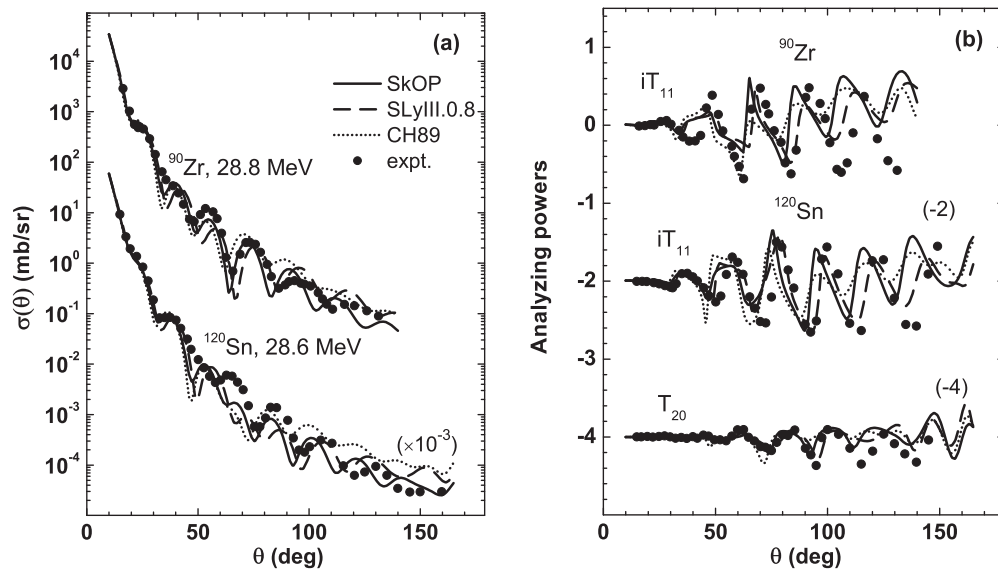


FIG. 2. Observables of the elastic deuteron scattering on ^{90}Zr at 28.8 MeV and ^{120}Sn at 28.6 MeV, calculated by the developed model of dA MOP. Experimental data are from Refs. [35,36].

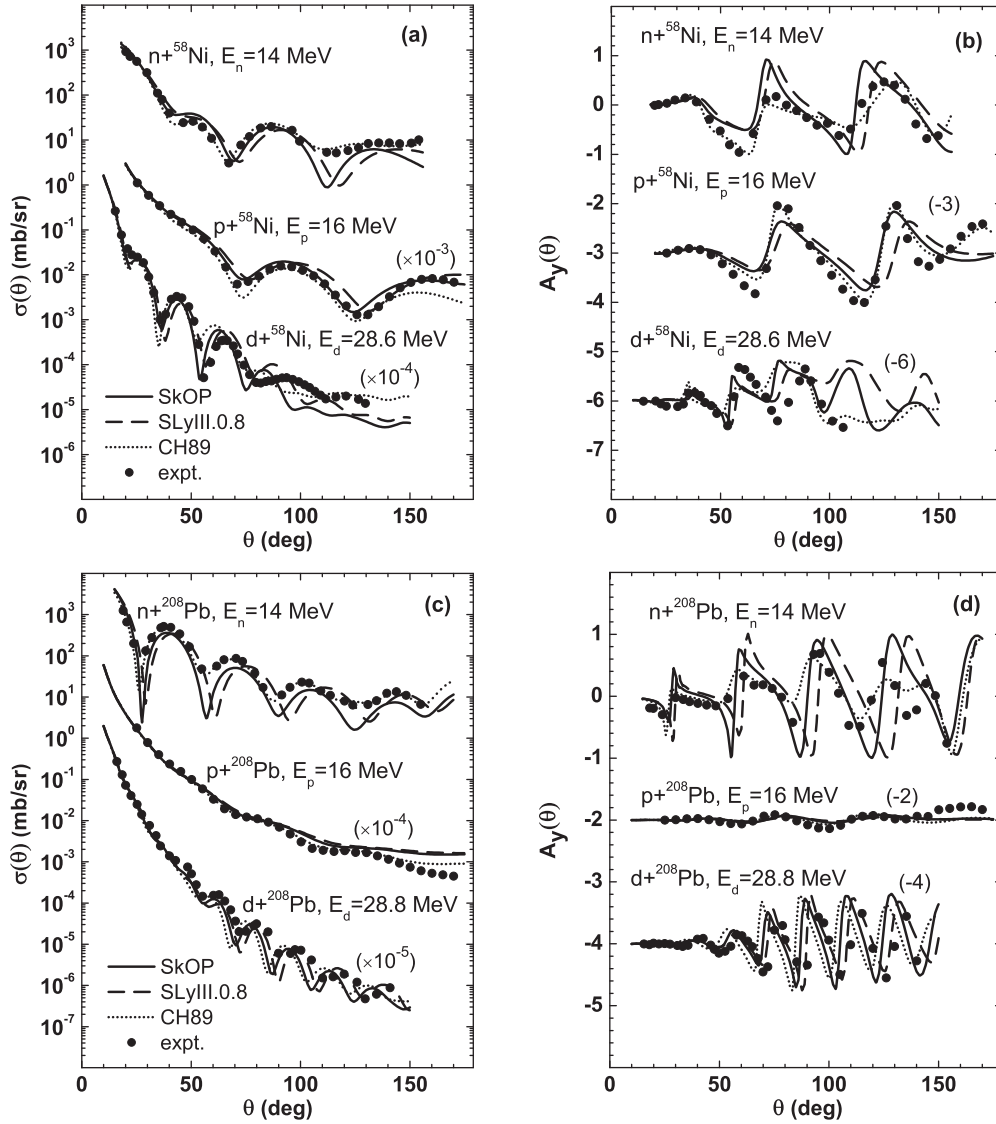


FIG. 3. Differential cross sections $\sigma(\theta)$ and analyzing powers $A_y(\theta)$ for the elastic scattering of deuterons at $E_d \approx 29$ MeV on ^{58}Ni and ^{208}Pb nuclei and of neutrons and protons on the same nuclei at the energy $E \approx E_d/2$, calculated by the considered models of NA and dA MOP. Experimental data are from Refs. [35,37–41].

nuclei, as well as for the tensor analyzing power $T_{20}(\theta)$ for the latter target nucleus, at the same energy value $E_d \approx 29$ MeV, as in Fig. 1. Like in the case of scattering on ^{208}Pb , here the description obtained in the considered model for the analyzing powers is somewhat better than for the cross sections, especially in the case of the ^{120}Sn target nucleus, and the calculations with the global NA potential CH89 do not give better results, as compared with the model based on the Skyrme forces.

Note that the SkOP force was found in Ref. [26] from fitting the differential cross section of $n + ^{116}\text{Sn}$ scattering at the neutron energy of $E = 14$ MeV. In the calculations of cross sections and polarization observables of the NA scattering in Refs. [25,26] on the basis of various Skyrme forces, the best description of experimental data was obtained at the neutron energies $E < 20$ MeV, and for the proton scattering this model yielded satisfactory results also at somewhat higher energy

values. However, in description of the proton scattering there arises a certain limitation of this model at small energies owing to the existence of the Coulomb barrier in the real pA potential, which is most essential for heavy target nuclei. Therefore, this model of NA MOP can be used for constructing the dA optical potential at energies lower than 50 MeV, because in this case it works well for describing both the neutron- and proton-nucleus scattering. Figure 3 presents the results of calculations of cross sections and analyzing powers for the elastic deuteron scattering on ^{58}Ni and ^{208}Pb nuclei at the energy $E_d \approx 29$ MeV, as well as for the neutron and proton scattering on the same nuclei at energy values close to the energy of nucleons in the incident deuteron ($E \approx E_d/2$). As can be seen, these calculations provide simultaneously a satisfactory description of observables of both the deuteron and nucleon scattering. Although the phenomenological potential CH89 gives a somewhat better description of the NA scattering

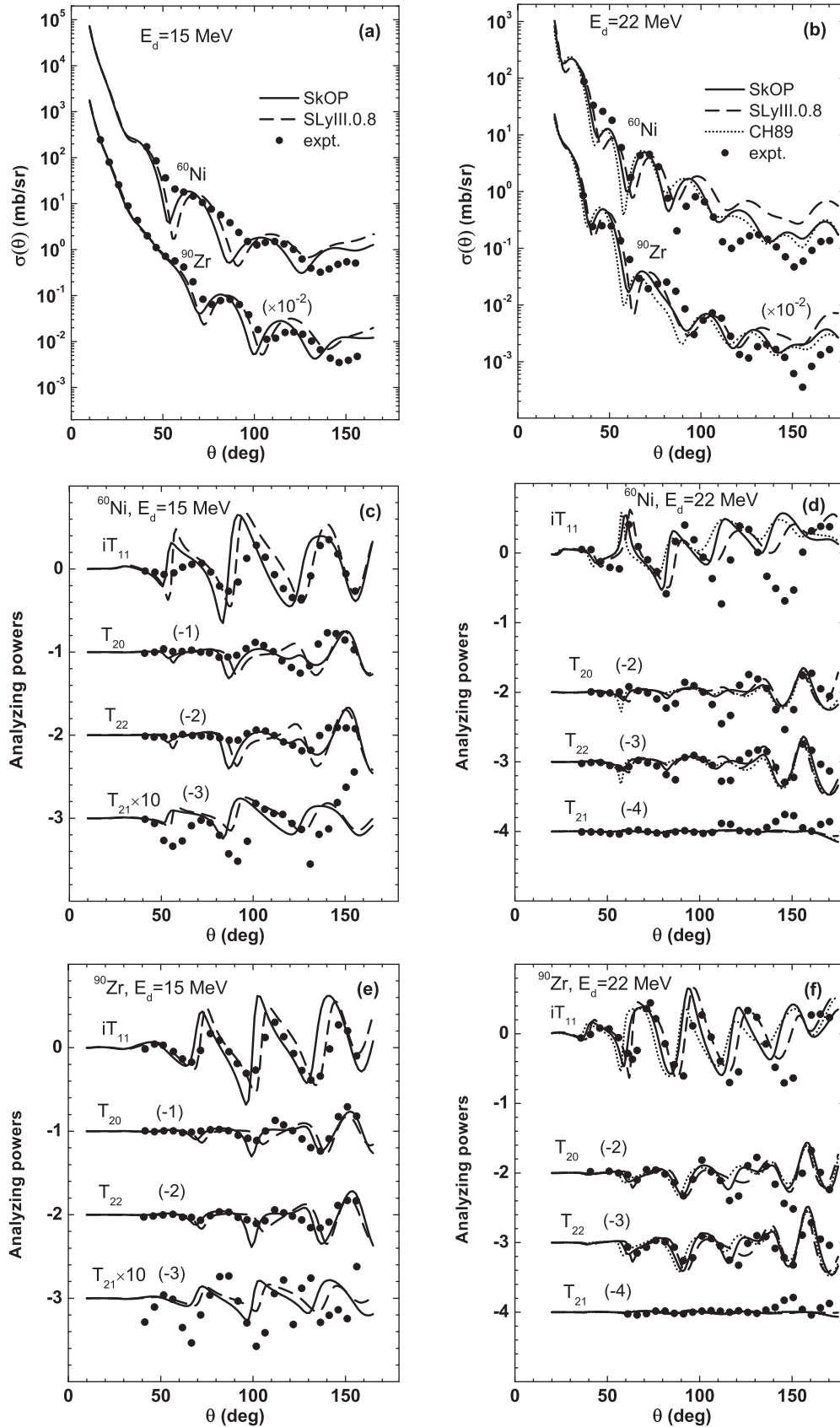


FIG. 4. Differential cross sections $\sigma(\theta)$, vector $iT_{11}(\theta)$, and tensor $T_{2m}(\theta)$ analyzing powers of the elastic deuteron scattering on ^{60}Ni and ^{90}Zr nuclei at 15 and 22 MeV. Experimental data are from Refs. [47,48].

than our microscopic model does, the quality of description of the deuteron scattering in Fig. 3 is roughly the same. Some shortcomings in describing the deuteron scattering can be explained by a number of simplifications made in the employed model of dA MOP.

In Fig. 4, we present the results of calculations of differential cross sections and vector and tensor analyzing powers for the elastic deuteron scattering on ^{60}Ni and ^{90}Zr nuclei at somewhat lower energy values of 15 and 22 MeV on the basis of the described model of dA MOP with using the Skyrme force variants SkOP and SLyIII.0.8 in comparison with the corresponding experimental data. The comparison with calculations on the basis of the global NA optical potential CH89 is made only at the energy value that belongs to the region of its determination ($E > 10$ MeV). On the whole, we may conclude that the model under consideration yields a reasonable description of the observables of dA scattering also in these cases. It should be noted that there is not altogether bad agreement with the experimental data for the calculated polarization observables. The best description is seen for the vector analyzing power $iT_{11}(\theta)$. As for the tensor analyzing powers, some shortcomings in the description of the quantities $T_{20}(\theta) = A_{zz}/\sqrt{2}$ and $T_{21}(\theta) = -A_{xz}/\sqrt{3}$ can be caused by the fact that in this variant of the model there is no tensor part of the dA MOP, which can be essential for describing the quantities A_{zz} and A_{xz} [6]. The calculations with the SLyIII.0.8 force give a description of the dA scattering that is comparable with the calculations with our optimized force SkOP, which ensured a better description of the neutron scattering. We also note that employing our optimized extended Skyrme force SkOP3 also yielded results, close to those for SkOP, and does not allow us to remove certain drawbacks in agreement of the calculated cross sections with the data. Note also that the results of calculations with the global NA optical potential CH89 do not look better than those with the used Skyrme forces.

Because in describing the dA scattering observables on the basis of the considered model there are certain discrepancies with experimental data, a question arises about a possible role of effects that have been neglected in this approximation. When describing the elastic scattering of such weakly bound nuclei as deuterons, in the incident-particle energy region under consideration an important role can be played by effects related to the influence of channels of deuteron virtual breakup. For this reason, in addition to using the main approximation in the form of the Watanabe-like model for the dA MOP, we have also estimated possible corrections to this approach, which are generated by contributions from such virtual channels.

At present, as one of the most accurate methods for describing scattering processes of deuterons with the allowance for their virtual breakup, the method of CDCC [10–13] is considered. Virtually, this approach allows one to take account of the contribution of the last term in Eq. (10), this equation being complemented by a set of equations describing inelastic channels coupled with the entrance one. In Ref. [9], the accuracy of the CDCC method was tested by means of comparison with calculations on the basis of solving the three-particle Faddeev equations.

To assess the effects of deuteron breakup in the CDCC approach, we have used the known numerical code FRESKO 2.9 [50]. In the calculations of scattering cross sections with the FRESKO code, as in Ref. [9], we did not take into account the spin-orbit interaction in Eq. (8) ($V_{SO,q} = 0$). In the FRESKO code, the deuteron wave functions in the ground state (the S wave) and in the continuum ($l = 0, 1, 2$) are taken for the Gauss potential: $V_{12}(r) = -v_0 \exp[-(r/r_0)^2]$ (with $v_0 = 72.15$ MeV and $r_0 = 1.484$ fm) in Eq. (2). For the discretization of continuum we used 10 bins with a uniform step in energy and did not allow for closed channels. The radius of matching was equal to 40 fm, the maximum angular momentum was 60, and the multipolarity of expansion of the potentials was 4. With these parameters for the FRESKO code, we were able to reproduce well all the results presented in Ref. [9] for the elastic dA scattering cross sections in the energy range from 12 up to 56 MeV calculated with employing the NA optical potential CH89.

In Fig. 5, we present a comparison of the results of calculations of the differential cross sections of the elastic deuteron scattering on $^{58,60}\text{Ni}$ nuclei at several energies performed by the CDCC method with the FRESKO code and in the Watanabe approximation with our code on the basis of the Skyrme forces SkOP and SLyIII.0.8, as well as for analogous calculations with using the NA potentials CH89. Note that the results of calculations in the Watanabe approximation by means of FRESKO and with our code (if the spin-orbit interaction is also omitted) are very close in spite of employing different deuteron wave functions in these codes. Generally, our calculations in this approximation with different variants of the deuteron wave function show a somewhat weak sensitivity to its choice in the energy region under consideration. From Fig. 5, one can see that the allowance for the effects of deuteron virtual breakup can yield certain noticeable corrections but it does not lead to changing radically the behavior of the calculated cross sections, and their influence somewhat increases with the deuteron energy growth, especially in the region of large scattering angles. It is interesting that the character of influence of these effects considerably differs in the calculations on the basis of the Skyrme forces and with using the NA potentials CH89; in the latter case they being more pronounced.

In Ref. [51], a new code for solving the equations in the CDCC approach was developed, and it was tested for the Gauss-potential wave functions, which showed a very good agreement with results obtained with the FRESKO code at the same calculation conditions. On the other hand, we have made a comparison of the results of calculations in the CDCC approach, using the global NA potential CH89, which have been carried out with FRESKO and were performed in the work of Ref. [51] with more realistic deuteron wave functions (for the Reid potential). This comparison shows sensitivity of the effects of deuteron breakup to the choice of the deuteron wave functions (see Fig. 6). The calculations with FRESKO that are shown in Fig. 6 have been performed by us at the same conditions, as in Ref. [51] (four bins with equal spacing, $l = 0, 2$, and the Coulomb dA potential from CH89 are used). It can be seen from Fig. 6 that this sensitivity increases with the incident deuteron energy. Here we also show the curves we have calculated by the FRESKO code, using the NA MOP with

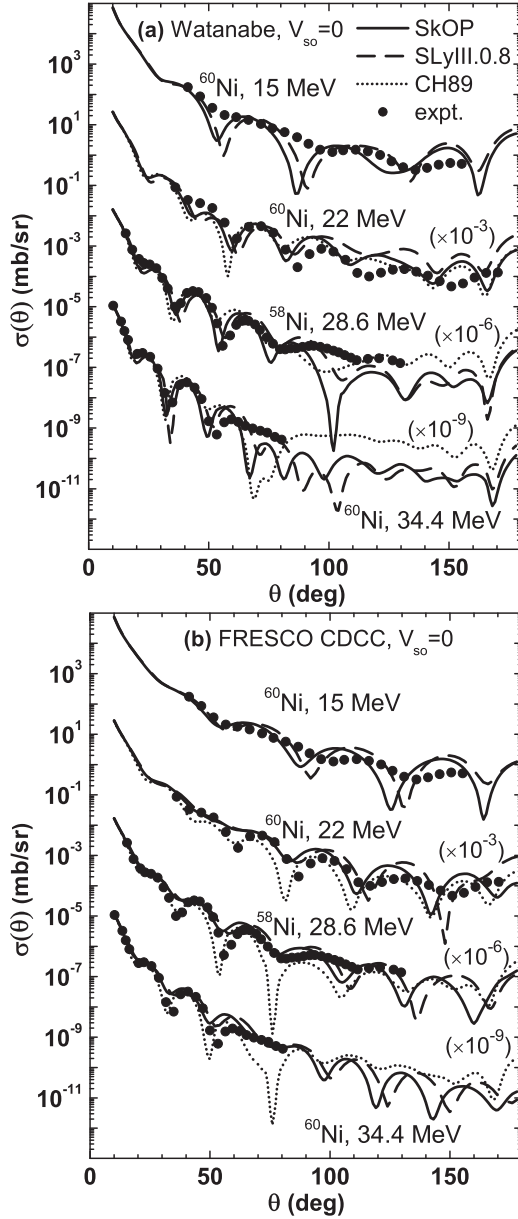


FIG. 5. Differential cross sections $\sigma(\theta)$ of the elastic deuteron scattering on $^{58,60}\text{Ni}$ nuclei at different energy values, calculated in the Watanabe approximation (a) and by CDCC (b) with the FRESKO code. Experimental data are from Refs. [37,47–49].

our Skyrme force SkOP. In Ref. [51], as also in our calculations with FRESKO, the spin-orbit interaction and the D wave in the deuteron ground-state wave function were not allowed for, which should be taken into account in a further more thorough analysis of the experimental data on the basis of the CDCC approach.

IV. CONCLUSION

We have considered an approach to constructing the microscopic optical dA potential for analyzing differential cross sections and polarization observables of the deuteron elastic scattering on even-even nuclei at medium energies on the basis of up-to-date effective Skyrme forces, including those

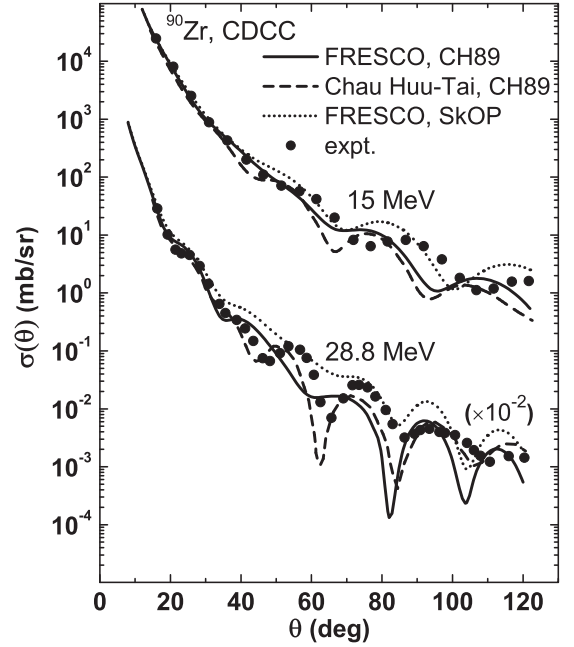


FIG. 6. Differential cross sections $\sigma(\theta)$ of the elastic deuteron scattering on ^{90}Zr nuclei at different energies, calculated in the CDCC approximation with deuteron wave functions for the Gauss (the FRESKO code) and Reid (the curve by P. Chau Hui-Tai from Ref. [51]) potentials. Experimental data are from Refs. [35,47].

of the extended form with allowance for both the momentum- and density-dependent terms, which provide simultaneously a satisfactory description of the nuclear structure in calculations by the Hartree-Fock method. We consider the description of the dA scattering in the three-body $n + p + A$ model with using the NA optical potentials, which were obtained earlier by the authors from simultaneously analyzing the elastic NA scattering observables and nuclear structure in a self-consistent microscopic approach with the Skyrme forces. The sought dA MOP, under neglecting the effects of deuteron virtual breakup, which corresponds to the well-known Watanabe model, was presented in the form of the folding of the deuteron wave function with these NA optical potentials. In this approximation, expressions have been found for the real and imaginary parts of the dA MOP for the case of using the above-mentioned variants of Skyrme forces.

In the considered approach, we have carried out an analysis of the differential cross sections and vector and tensor polarization observables at the deuteron energies $E_d < 50$ MeV in a wide range of the mass numbers of target nuclei (from ^{58}Ni up to ^{208}Pb) with using both the well-approved up-to-date standard and extended Skyrme forces from the literature, as well as the NN force variants optimized by us. The calculations show that employing the developed model of dA MOP with making use of some of the considered standard-form Skyrme force variants from the literature, as well as the optimized NN force variants of the standard and extended types proposed by the authors, provides a reasonable description of experimental data for the differential cross sections and vector and some of tensor analyzing powers of the elastic dA scattering by different target nuclei in this energy

region. The description of the set of tensor analyzing powers probably could be improved by allowance for the tensor part of dA MOP, which was neglected here.

In addition to the calculations in the main approximation in the form of the Watanabe-type model, we have also performed estimations of possible contributions of the effects related to deuteron virtual breakup channels. An analysis of such corrections was performed in calculations of differential cross sections of the elastic dA scattering in the CDCC approach with employing the known numerical code FRESKO 2.9. The conclusion was made that the allowance for deuteron breakup in the energy region under consideration sometimes can give noticeable corrections, but does not lead to a cardinal change of the results of calculations of scattering observables by the considered model based on the Skyrme forces.

The results of the calculations performed show that the employment of the self-consistent approach based on the

effective Skyrme NN forces for describing processes of the nucleon and deuteron scattering on nuclei in the microscopic optical model leads to reasonable results, along with a successful description of the nuclear structure by the SHF method with the same Skyrme forces. However, because in describing the dA scattering observables on the basis of the considered model there are certain discrepancies with experimental data, it is necessary to thoroughly investigate a possible role of different effects that have been neglected in the approach used. In particular, it is advisable to take into account the D wave in the deuteron wave function, which would lead to the rise of the tensor part of the dA MOP, and to perform much more accurate allowance for the deuteron breakup effects with employing more realistic deuteron wave functions, presumably, in the CDCC approach. It also would be necessary to investigate the role of effects related to going beyond the three-body $n + p + A$ model.

-
- [1] M. E. Brandan and G. R. Satchler, *Phys. Rep.* **285**, 143 (1997).
 [2] K. Amos, P. J. Dortmans, H. V. von Geramb, S. Karataglidis, and J. Raynal, in *Advances in Nuclear Physics*, edited by J. W. Negele and E. Vogt, Vol. 25 (Plenum, New York, 2000), p. 275.
 [3] J. Cook, *Nucl. Phys. A* **382**, 61 (1982).
 [4] S. Watanabe, *Nucl. Phys.* **8**, 484 (1958).
 [5] F. Perey and G. Satchler, *Nucl. Phys. A* **97**, 515 (1967).
 [6] N. Matsuoka, H. Sakai, T. Saito, K. Hosono, M. Kondo, H. Ito, K. Hatanaka, T. Ichihara, A. Okihana, K. Imai, and K. Nisimura, *Nucl. Phys. A* **455**, 413 (1986).
 [7] M. Avrigeanu, H. Leeb, W. von Oertzen, F. Roman, and V. Avrigeanu, in *Proceedings of the International Conference on Nuclear Data for Science and Technology, Nice, 2007*, edited by O. Bersillon, F. Gunsing, E. Bauge, R. Jacqmin, and S. Leray (EDP Sciences, Paris, 2008), p. 219.
 [8] A. Deltuva, *Phys. Rev. C* **79**, 021602 (2009).
 [9] N. J. Upadhyay, A. Deltuva, and F. M. Nunes, *Phys. Rev. C* **85**, 054621 (2012).
 [10] R. C. Johnson and P. J. R. Soper, *Phys. Rev. C* **1**, 976 (1970).
 [11] G. H. Rawitscher, *Phys. Rev. C* **9**, 2210 (1974).
 [12] N. Austern, Y. Iseri, M. Kamimura, M. Kawai, G. H. Rawitscher, and M. Yahiro, *Phys. Rep.* **154**, 125 (1987).
 [13] M. Yahiro, Y. Iseri, H. Kameyama, M. Kamimura, and M. Kawai, *Prog. Theor. Phys. Suppl.* **89**, 32 (1986).
 [14] N. K. Timofeyuk and R. C. Johnson, *Phys. Rev. Lett.* **110**, 112501 (2013).
 [15] N. K. Timofeyuk and R. C. Johnson, *Phys. Rev. C* **87**, 064610 (2013).
 [16] R. C. Johnson and N. K. Timofeyuk, *Phys. Rev. C* **89**, 024605 (2014).
 [17] R. C. Johnson, *J. Phys. G* **41**, 094005 (2014).
 [18] D. Vautherin and D. M. Brink, *Phys. Rev. C* **5**, 626 (1972).
 [19] M. Dutra, O. Lourenço, J. S. Sá Martins, A. Delfino, J. R. Stone, and P. D. Stevenson, *Phys. Rev. C* **85**, 035201 (2012).
 [20] Q.-B. Shen, Y.-I. Han, and H.-R. Guo, *Phys. Rev. C* **80**, 024604 (2009).
 [21] Y. Xu, H. Guo, Y. Han, and Q. Shen, *J. Phys. G* **41**, 015101 (2014).
 [22] V. I. Kuprikov, V. V. Pilipenko, A. P. Soznik, V. N. Tarasov, and N. A. Shlyakhov, *Phys. At. Nucl.* **72**, 975 (2009).
 [23] V. V. Pilipenko, V. I. Kuprikov, and A. P. Soznik, *Nucl. Phys. At. Energy* **11**, 367 (2010).
 [24] V. V. Pilipenko, V. I. Kuprikov, and A. P. Soznik, *Phys. Rev. C* **81**, 044614 (2010).
 [25] V. V. Pilipenko and V. I. Kuprikov, *Phys. Rev. C* **86**, 064613 (2012).
 [26] V. I. Kuprikov and V. V. Pilipenko, *Phys. At. Nucl.* **76**, 113 (2013).
 [27] S. Krewald, V. Klemt, J. Speth, and A. Faessler, *Nucl. Phys. A* **281**, 166 (1977).
 [28] M. Farine, J. M. Pearson, and E. Tondeur, *Nucl. Phys. A* **615**, 135 (1997).
 [29] S. Goriely, N. Chamel, and J. M. Pearson, *Phys. Rev. C* **82**, 035804 (2010).
 [30] H. Guo, Y. Xu, Y. Han, and Q. Shen, *Phys. Rev. C* **81**, 044617 (2010).
 [31] V. I. Kuprikov, V. V. Pilipenko, and A. P. Soznik, *Phys. At. Nucl.* **75**, 832 (2012).
 [32] D. J. Thouless, *The Quantum Mechanics of Many-Body Systems* (Academic Press, New York, 1972).
 [33] C. B. Dover and N. Van Giai, *Nucl. Phys. A* **190**, 373 (1972).
 [34] R. C. Johnson and P. J. R. Soper, *Nucl. Phys. A* **182**, 619 (1972).
 [35] R. Röche, N. V. Sen, G. Perrin, J. C. Gondrand, A. Fiore, and H. Müller, *Nucl. Phys. A* **220**, 381 (1974).
 [36] G. Perrin, N. Van Sen, J. Arvieux, C. Perrin, R. Darves-Blanc, J. L. Durand, A. Fiore, J. C. Gondrand, and F. Merchez, *Nucl. Phys. A* **206**, 623 (1973).
 [37] G. Perrin, N. Van Sen, J. Arvieux, R. Darves-Blanc, J. L. Durand, A. Fiore, J. C. Gondrand, F. Merchez, and C. Perrin, *Nucl. Phys. A* **282**, 221 (1977).
 [38] P. P. Guss, R. C. Byrd, C. E. Floyd, C. R. Howell, K. Murphy, G. Tungate, R. S. Pedroni, R. L. Walter, J. P. Delaroche, and T. B. Clegg, *Nucl. Phys. A* **438**, 187 (1985).
 [39] R. L. Varner, Ph.D. thesis, University of North Carolina, 1986.
 [40] C. E. Floyd Jr., Ph.D. thesis, Duke University, 1981.

- [41] C. E. Floyd, P. P. Guss, K. Murphy, C. R. Howell, R. C. Byrd, G. Tungate, S. A. Wender, R. L. Walter, and T. B. Clegg, *Phys. Rev. C* **25**, 1682 (1982).
- [42] A. Pastore, D. Davesne, K. Bennaceur, J. Meyer, and V. Hellemans, *Phys. Scr.* **T154**, 014014 (2013).
- [43] K. Washiyama, K. Bennaceur, B. Avez, M. Bender, P.-H. Heenen, and V. Hellemans, *Phys. Rev. C* **86**, 054309 (2012).
- [44] X. Roca-Maza, G. Colò, and H. Sagawa, *Phys. Rev. C* **86**, 031306(R) (2012).
- [45] S. Goriely, N. Chamel, and J. M. Pearson, *Phys. Rev. C* **88**, 024308 (2013).
- [46] R. L. Varner, W. J. Thompson, T. L. McAbee, E. J. Ludwig, and T. B. Clegg, *Phys. Rep.* **201**, 57 (1991).
- [47] H. R. Bürgi, W. Grüebler, J. Nurzynski, V. König, P. A. Schmelzbach, R. Risler, B. Jenny, and R. A. Hardekopf, *Nucl. Phys. A* **321**, 445 (1979).
- [48] M. Takei, Y. Aoki, Y. Tagishi, and K. Yagi, *Nucl. Phys. A* **472**, 41 (1987).
- [49] E. Newman, L. C. Becker, and B. M. Freedom, *Nucl. Phys. A* **100**, 225 (1967).
- [50] I. J. Thompson, *Comput. Phys. Rep.* **7**, 167 (1988).
- [51] P. Chau Huu-Tai, *Nucl. Phys. A* **773**, 56 (2006).